Preprints of the 19th World Congress
The International Federation of Automatic Control
Cape Town, South Africa. August 24-29, 2014

Robust impedance active control of flight control devices

J.P. Condomines * **F. Defay** * **D. Alazard** *

* *Institut Supérieur de l'Aéronautique et de l'Espace, Toulouse, France (e-mail: [f.defay, d.alazard,j-p.condomines]@ isae.fr).*

Abstract: This paper focuses on the control of the mechanical impedance of an aircraft yoke. The control architecture involves an inner position servo-loop and an outer loop feedbacking the torque/force measurement to the position reference input through the required admitance model. Two different approaches are presented for the inner position servo-loop design: a classical Proportional-Derivative control and a structured H_∞ control. These two approaches are compared from the performance/robustness trade off point of view. The performance and robustness indexes are respectively the maximal variation on the required admittance model and the maximal pilot own impedance supported by the closed loop system before to become unstable. These indexes are computed using real μ-analysis. Both approaches are implemented on an experimental test-bed. Analysis and exprimental results with a pilot in the loop confirm that the structured H_∞ controller is the best solution.

Keywords: Robust control, haptic interfaces, robustness analysis, μ-analysis.

1. INTRODUCTION

In the past, pilots had to use their own physical strength to control aircraft since their yokes and rudder pedals were directly connected to control surfaces by cables. Therefore, the pilot felt exactly what happened during the flight. Gradually, when the performance and the size of aircraft increased, hydraulic actuators were added to the aircraft's control systems to facilitate piloting, especially after the implementation of digital control systems. Thus, the pilot has no more direct link with the control surfaces. In fact, on-board computers and avionics are used as the intermediate between the pilot and control surfaces. It seems that this technology brings greater accuracy, security and makes the flight more comfortable. However, the pilot has then lost the feeling provided by traditional devices.

To overcome this problem, an active device with force feedback can be used to control the device mechanical impedance felt by the pilot. Such an active device can be also used to feedback kinesthetic sensations for the pilot according to the operational state of the aircraft. This technology gives a lot of advantages in terms of the weight, the volume, the assembly time and the number of components to be installed by removing e.g. mechanical links and beams used to couple pilot and co-pilot control devices.

The force feedback problem is well established in tele-operation in medical, automotive industry and more generally in the context of haptic interfaces. To control Human machine interface, impedance control is often used to assist the human or interact with them [1] [2]. Several robotic applications require to take into account the impedance of the operators [3] [4].

The specific aspect of the active feedback for the flight control device is not described yet in the literature and its application is not actually done on aircraft. The overall aim of this project is to control in real time the mechanical impedance of the device in order to adapt its apparent inertial, stiffness and damping. Such a closed-loop force controlled device will allow :

- to adjust the impedance to the morphology of the pilot or to the wish of the pilot or the company;
- to give some kinesthetic sensations to the pilot in order to inform him on the operational state of the aircraft (e.g. near the boundaries of the flight envelope);
- to couple the pilot and copilot yokes or choose the more importance between them in detecting their behaviors;
- to evaluate the impact of such a system on human factors (tolerance to defects, pilot fatigue, etc).

The control laws must be robust agains disturbances and uncertainties in order to the closed-loop system to be safe. The principal disturbance on the active feedback is well known, that's the interaction with the pilot's own impedance [5]. For a flight control device, it is essential to control its impedance in order to support all possible pilot behaviors (stress, drowsiness , tension, etc). In this paper, variations on the pilot's own inertia are considered. The damping and stiffness of the pilot are assumed to be constant. Indeed, variations on the pilot/device inertia appear to be the most sensitive source of disturbances for impedance control laws [6] [8].

An experimental test-bench composed of two identical and active yokes was developed to illustrate and validate some various control concepts. In [9], control laws of couple pilot and co-pilot devices were presented. The proposed

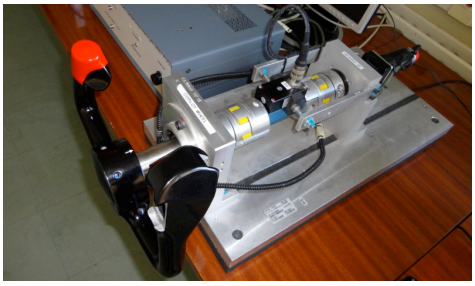

Fig. 1. Active yoke demonstrator

control law architecture involves an inner angular servo-loop position with a wide bandwidth and an outer loop which feedback the torque measurement to the position reference input through a reference admittance. In [10], this experimental device is used with a full flight simulator to validate the intersest of active feedback system for aircraft guidance.
In this paper, the design of the inner position servo-loop is reconsidered by using two different approaches: a classical proportional-derivative design and a structured low-order H_∞ design. μ-analysis is then applied to both designs to evaluate the robustness in terms of admissible variations on pilot's inertia and performance in terms of admissible range on prescribed apparent admittance.

The main contributions of this paper are : (i) the use of structured H_∞ controller tools to design a low-order impedance controller which can be comparable to the classical one from the complexity point of view and easily implementable, (ii) the use of real μ-analysis to evaluate the operating domain of the closed-loop system in terms of admissible variations on the required apparent admittance and its parametric robustness to pilot's inertia. The specific feature of this application is not addressed in previous works in the field of tele-operation or steering by wire. Both control designs and μ-analysis results are validated on the exprimental test-bench.

The article is structured as follows: In Section II, the model of the experimental test-bench and the control objectives are presented. In section III, the control structure and the design of proportional-derivative are detailed. Moreover experimental results are presented and a first μ-analysis is done. In section IV, the H_∞ standard problem is depicted and section V shows experimental results of the robust controller.

2. MODEL AND OBJECTIVES

The experimental setup (see Fig. 1) is used here to illustrate an one-degree of freedom aircraft yoke with artificial feedback to the pilot. In this system, the main components are a brushless DC motor fitted with a position sensor, a gear train (AF/AFR series, back-drivable) with a ratio $n = 100$ and a torque sensor (DR2208) linked to the gear train ouput and the yoke mounted by two mechanical coupling joints (ROTEX GS). The strain gauges of the torque sensor introduces a stiffness k. J_y denote the inertia of the yoke and J_m stands for the motor inertia seen from the gear train output ($J_m = J_m^i\, n^2$). A simplified linear spring string-mass model shown in Fig. 2 can be used to represent the system with the following assumptions: (a) the human

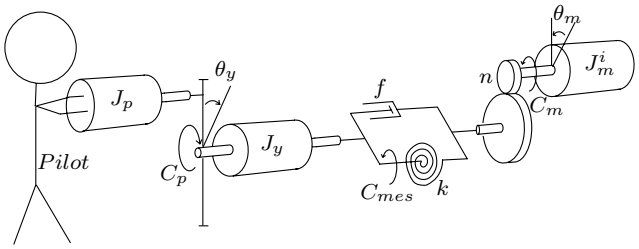

Fig. 2. Simplified mechanical model.

arm can be considered as a pure inertia denoted J_p (see section III-A); (b) the low damping coefficient f represent all frictions (motor/transducer and strain gauges). The following notations will be used :

- C_{mes} : torque measured by the torque-meter;
- θ_y : yoke angular position measured by a potentiometer;
- θ_m : motor angular position measured by the resolver;
- C_p : pilot torque applied on the yoke;
- C_m : motor torque (command input).

The model $G(s)$ betwen the 2 inputs (C_p, C_m) and the 3 outputs (θ_y, θ_m, C_{mes}) can be described by the state space representation (1).

$$G(s): \begin{cases} \dot{x} = \begin{bmatrix} 0 & 0 & 1 & 0 \\ 0 & 0 & 0 & 1 \\ \frac{-k}{J_y} & \frac{k}{J_y} & \frac{-f}{J_y} & \frac{f}{J_y} \\ \frac{k}{J_m} & \frac{-k}{J_m} & \frac{f}{J_m} & \frac{-f}{J_m} \end{bmatrix} x + \begin{bmatrix} 0 & 0 \\ 0 & 0 \\ \frac{1}{J_y} & 0 \\ 0 & \frac{1}{J_m} \end{bmatrix} u \\ y = \begin{bmatrix} 1 & 0 & 0 & 0 \\ 0 & 1 & 0 & 0 \\ k & -k & 0 & 0 \end{bmatrix} x \end{cases} \tag{1}$$

where : $x = [\theta_y \;\; \theta_m \;\; \dot{\theta}_y \;\; \dot{\theta}_m]^T$, $u = [C_p \;\; C_m]^T$ and $y = [\theta_y \; \theta_m \; C_{mes}]$

Some experiments have been carried out to identify the system dynamic parameters [9],[10]: $k = 800 N.m/rad$; $f = 2.5\, Nm.(rad/sec)$; $J_m = 16.10^{-2} kg.m^2$; $J_y = 3.10^{-2} kg.m^2$. $G_d(z)$ is the continuous-to-discrete time conversion of $G(s)$ and the various controllers are implemented in Matlab/Simulink xPCtarget environment and executed on the Real-Time Application Interface.

The first objective (**objective #1**) is to design a controller for shaping the yoke mechanical impedance $Z_y(s)$ (felt by the pilot) according to a reference impedance model denoted $Z_{ref}(s)$. Thereby, $Z_y(s) = \frac{C_p(s)}{\theta_y(s)}$ represent the transfer function between the yoke position θ_y and the pilot torque C_p. The admittance is defined as $Y_{ref}(s) = Z_{ref}^{-1}(s) = \frac{1}{J_a.s^2 + D_a.s + K_a}$ where J_a, D_a and K_a are the required apparent inertia, damping and stiffness of the yoke, respectively. To increase the operating capabilities, the controller must support variations on these required apparent parameters. The main objective is to decrease the apparent inertia to $J_a = 0.1\, kg.m^2$, i.e. two

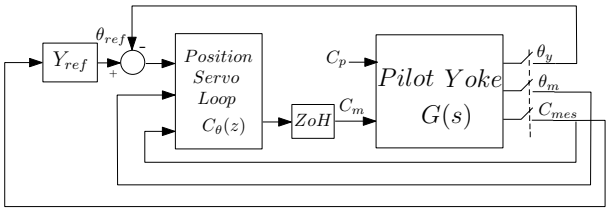

Fig. 3. Control architecture based on the admittance control with position feedback G_{cl}.

times "lighter" than the natural total device inertia ($J_m + J_y = 0.19\,kg.m^2$), in order to improve maneuverability. The objective to decrease the apparent inertia of haptic devices is also adressed in [11], using a feedforward approach.

The second objective (**objective #2**) concerns the robustness of the haptic device to uncertainties on human arm inertia. Indeed, it was shown in [9] that unstabilized coupling between the pilot and the device may occur in case of a low prescribed apparent inertia J_a. Both objectives (**objective #1** and **objective #2**) will be evaluated using μ-analysis which is the method chosen in our case.

3. ADMITTANCE CONTROL

The *admittance control with position feedback* terminology will be used to avoid the confusion with the impedance controller. This type of control consists of two control loops: an outer loop to control the admittance (i.e. the inverse of the impedance) and a inner position servo loop. Thus, the discrete-time control architecture involving yoke models is depicted in Fig. 3 where an inner position servo-loop involves the controller $C_\theta(z)$. If the position input reference θ_{ref} is set to 0 (i.e. $Y_{ref}(s) = 0$), then the position servo-loop rejects external disturbances including the pilot torque C_p. Such a solution is called minimal admittance (or maximal impedance) in [9]. The admittance reference model $Y_{ref}(z)$ and $C_\theta(z)$ are obtained from $Y_{ref}(s)$ and $C_\theta(s)$ by a continuous to discrete time TUSTIN conversion.

Inside the position servo loop bandwidth ($\geq 100\,rad/s$), we can assume that $C_{mes} \approx C_p$. Such a bandwidth is wider than the neural control loop bandwidth of the pilot [12]. Then, (**objective #1**) can be simply met by returning the measured torque C_{mes} to the position input reference θ_{ref} through the admittance reference model Y_{ref}.

3.1 PD control of the position inner loop

$C_\theta(z)$ is made up of a proportional gain K_p on the tracking error $(\theta_{ref} - \theta_y)$ and a derivative gain K_v on the motor angular rate and be written as :

$$C_m = K_p(\theta_{ref} - \theta_y) - K_v \frac{z-1}{z - e^{-\tau.T_s}}\theta_m + 0.C_{mes} \quad (2)$$

The position servo-loop performances, and thus the two gains K_p and K_v, are limited by the transmission compliance and the sampling period [13]. Note that C_{mes} is not used implemented in the feedback. The design of a dynamic feedback using C_{mes} will be tackled only in the H_∞ design (see section IV), this constitutes a limitation of the comparison of this paper. A good trade-off performance/stability [14] is achieved for $K_p = 150\,Nm/rad$ and $K_v = 4.8\,Nms/rad$.

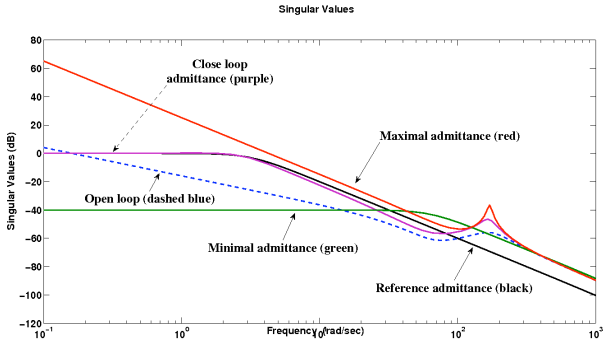

Fig. 4. Yoke admittance frequency-domain responses $\frac{\theta_y}{C_p}(s)$ for PD controller : open-loop (dashed blue), minimal admittance or closed-loop with $Y_{ref} = 0$ (green), maximal admittance (red), admittance reference model $Y_{ref}(s) = 1/(0.1s^2 + 0.44s + 1)$ (black), closed loop with admittance reference model (purple).

The Fig. 4 shows the singular values of the yoke admittance in open-loop (dashed blue plot) and in closed loop when $Y_{ref}(z) = 0$ (i.e. minimal admittance solution, green plot). The maximal admittance solution (i.e when $Y_{ref}(z) = 1/J_a s^2$ with a minimal apparent inertia J_a, see [9]) is depicted by the red line. Obviously, the magnitude of $Y_{ref}(s)$ is limited by the outer loop stability. Qualitatively, this control structure supports any admittance model $Y_{ref}(s)$ whose low frequency response is inside the area bounded by the minimal (green) and maximal (red) admittance responses in Fig. 4. For $Y_{ref}(s) = 1/(0.1s^2 + 0.44s+1)$ (black plot), the obtained yoke admittance, once the outer loop is closed, is the purple plot in Fig. 4. The obtained yoke admittance is therefore quite close to the reference model for low frequencies (up to 10 rad/s).

3.2 Closed-loop system performance without pilot

The evaluation of the performances of the closed loop system G_{cl} and the exprimental validation (within the useful operating conditions) were done by following procedure. When the yoke is free (no pilot) : i) a step function is added to the torque measuement C_{mes}, ii) the yoke position response $\theta_y(t)$ and its rise time are reccorded for different values of the reference admittance. More precisely, the apparent stiffness and damping are fixed ($K_a = 1N.m/rad$ and $D_a = 0.44\,Nms/rad$) while the apparent inertia J_a varies from $0.1\,kg.m^2$ to $1\,kg.m^2$. Fig. 5 represents the rise time of the system with respect to the apparent inertia J_a. Furthermore, the Fig. 6 gives us the steady state error for a constant apparent inertia $J_a = 1\,kg.m^2$ when the apparent stiffness K_a varies from $0.7\,Nm/rad$ to $4\,Nm/rad$. These figures show good reference tracking peformances and small errors between simulation and real systems and then validate the design model $G(s)$.

3.3 Dynamic coupling with pilot bio-impedance

The control structure proposed in Fig. 3 is quite interesting because it allows a large range of admittance reference model to be taken into account. For very low apparent

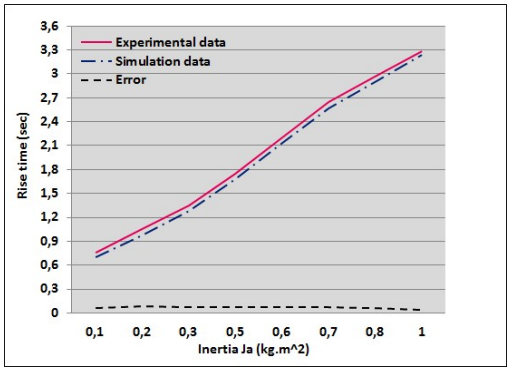

Fig. 5. Rise time vs apparent inertia (J_a): simulation and real experiment comparison.

inertia J_a in reference models, some dynamic couplings with the pilot's impedance can destabilize the system [9]. Although the torque is measured in the proposed control strategy (Fig. 3), the pilot cannot be considered as a pure torque generator. The pilot's impedance acts as an external feedback on the control device. The Fig. 7 shows the angular position of yoke $\theta_y(t)$ (black plot) when the pilot makes a solicitation. For $J_a = 0.1\,kg.m^2$ (performance objective), the reference position $\theta_{ref}(t)$ is in dashed blue plot. It is noticeable that the system is unstable when the pilot clenches the yoke at $time = 7.5sec$. Finally the motor current becomes too large and activates the security switch. Also, the result shows that the delay is not negligible ($0.1sec$) between $\theta_{ref}(t)$ and $\theta_y(t)$.

Stability problems for linear haptic interfaces (and in particular due to the human arm impedance) are also addressed in[14]. The exact modeling of the operator arm impedance is a complex problem [15] which takes into account the internal muscle length, nerve excitation of the α-neuron, feed-forward control of muscle length and force acting on the muscle. In general this impedance is defined by the relation Z_p =force/velocity. A simple model is given in[16] as a function of the second order: $Z_p = \frac{K_p}{s} + D_p + J_p s$. Where K_p, D_p and J_p are respectively the stiffness, damping and inertia of the operator arms. In [17], the damping D_p is estimated to be around $5.5Ns/m$ and the stiffness K_p varies in a large range (from $2Nm/rad$ to $400Nm/rad$). Lastly, the moment of inertia J_p is very uncertain because of the high sensitivity on how

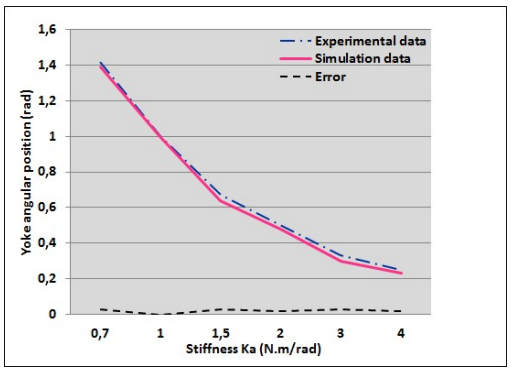

Fig. 6. Steady state vs apparent stiffness (K_a): simulation and real experiment comparison.

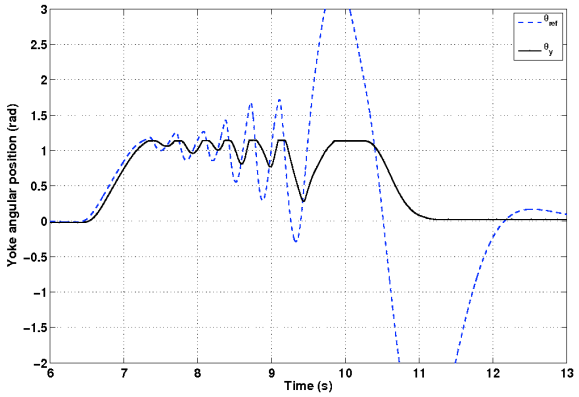

Fig. 7. Angular reference position of yoke (dashed blue line) and angular position of yoke (black line) when the pilot makes a sollicitation : $Y_{ref}(s) = 1/(0.1s^2 + 0.44s + 1)$.

the yoke is held. Regardless the model, the inertia of the pilot J_p increases considerably the inertia of the yoke J_y by the HUYGEN theorem and destabilizing the system. Priliminary analysis [9] have shown that the system stability is more sensitive to pilot inertia rather than other parameters (damping and stiffness). Thus, the robustness to pilot impedance model Z_p is restricted to variations on J_p.

3.4 Robustness analysis

The robust performance analysis of the closed loop system aims to compute the maximal admissible variation δ_{J_a} of the apparent inertia (performance) and the maximal admissible variation δ_{J_p} of the pilot inertia (robustness) for the closed-loop system to be stable. δ_{J_a}, δ_{J_p} are relative variations w.r.t. nominal values J_{a_0} and J_{p_0} and defined such as:

$$J_a = J_{a_0}(1 + \delta_{J_a}) \quad \text{and} \quad J_y + J_p = J_y(1 + \delta_{J_p}) \,. \tag{3}$$

Indeed $J_{p_0} = 0$ and the pilot inertia is added to the nominal yoke inertia J_y. Taking into account (3) in the closed-loop sketch (Fig. 3), the varying closed-system $\mathcal{S}(\delta_{J_a}, \delta_{J_p})$ can be described by the sketch of Fig. 8. The varying pilot yoke and the varying reference admittance are described by the following LFT (Linear Fractional Transformation):

- For the yoke model:

$$\begin{bmatrix} \dot{\theta_y} \\ \dot{\theta_m} \\ \ddot{\theta_y} \\ \ddot{\theta_m} \\ \hline z_1 \\ \theta_y \\ \theta_m \\ C_{mes} \end{bmatrix} = \left[\begin{array}{cccc|ccc} 0 & 0 & 1 & 0 & 0 & 0 & 0 \\ 0 & 0 & 0 & 1 & 0 & 0 & 0 \\ \frac{-k}{J_y} & \frac{k}{J_y} & \frac{-f}{J_y} & \frac{f}{J_y} & -1 & \frac{-k}{J_y} & 0 \\ \frac{k}{J_m} & \frac{-k}{J_m} & \frac{f}{J_m} & \frac{-f}{J_m} & 0 & 0 & \frac{1}{J_m} \\ \hline \frac{-k}{J_y} & \frac{k}{J_y} & \frac{-f}{J_y} & \frac{f}{J_y} & -1 & \frac{-k}{J_y} & 0 \\ 1 & 0 & 0 & 0 & 0 & 0 & 0 \\ 0 & 1 & 0 & 0 & 0 & 0 & 0 \\ -k & k & 0 & 0 & 0 & 0 & 0 \end{array}\right] \begin{bmatrix} \theta_y \\ \theta_m \\ \dot{\theta_y} \\ \dot{\theta_m} \\ \hline w_1 \\ C_p \\ C_m \end{bmatrix}$$

$$w_1 = \delta_{J_p} z_1 \,.$$

- For reference admittance :

$$\begin{bmatrix} \dot{\theta}_{ref} \\ \ddot{\theta}_{ref} \\ \hline \theta_{ref} \\ z_2 \end{bmatrix} = \left[\begin{array}{cc|cc} 0 & 1 & 0 & 0 \\ -\frac{K_a}{J_{a_0}} & -\frac{D_a}{J_{a_0}} & \frac{1}{J_{a_0}} & \frac{-1}{J_{a_0}} \\ \hline 1 & 0 & 0 & 0 \\ -K_a & -D_a & 1 & -1 \end{array}\right] \begin{bmatrix} \theta_{ref} \\ \dot{\theta}_{ref} \\ \hline C_{mes} \\ w_2 \end{bmatrix}$$

$$w_2 = \delta_{J_a} z_2 \,.$$

From these LFT and the controller $C_\theta(s)$, the $M(s)-\Delta$ form where $\Delta = \begin{bmatrix} \delta_{J_p} & 0 \\ 0 & \delta_{J_a} \end{bmatrix}$ required to apply μ-analysis can be easily derived. The μ-analysis is performed in the continuous-time domain, therefore the ZoH is not neglected in this analysis. Only the basic principles of μ-analysis are presented in this section [18]. At each frequency ω, μ-analysis computes an upper bound $\bar{\mu}(\omega)$ and a lower bound $\underline{\mu}(\omega)$ of the structured singular value μ. The μ-upper bound provides a robust stability guarantee, i.e :

$$\mathcal{S}(\delta_{J_p}, \delta_{J_a}) \text{ is stable} \quad \forall\, \delta_i \;/\; |\delta_i| \leq \frac{1}{\max_\omega \bar{\mu}(\omega)}\,, \quad i = J_p, J_a\,,$$

while μ-lower bound provides the worst-case parametric configuration $(\delta_{J_p}^{worst}(\omega),\ \delta_{J_a}^{worst}(\omega))$.

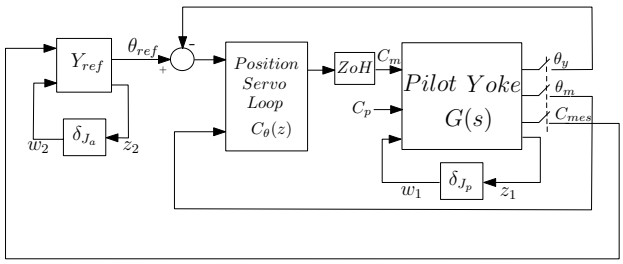

Fig. 8. System in the presence of parametric variations : $\mathcal{S}(\delta_{J_a}, \delta_{J_p})$

The main drawback of the μ-analysis is that $\mu(\omega)$ is computed on a frequency mesh. To determine accurately the μ frequency response peak, the mesh must be refined dynamically, especially in case of the system with flexible modes. In addition, the calculation of the lower bound of μ is NP hard. Two algorithms can be used to calculate in polynomial time an upper bound of μ in the case of real uncertainty. The first is based on solving LMIs (Linear Matrix Inequations) and the second is based on the minimization of singular value. Here, a recent Toolbox developed by [G. Ferreres and J-M Biannic] allows the mesh to be refined automatically to frame the μ upper-bound peak [19]. For $J_y = 0.03\,kg.m^2$ and $J_{a_0} = 1\,kg.m^2$ (nominal values), Fig. 9 plots μ upper and lowed bound responses on a mesh of 2000 points distributed between 0.1 and $200\,rad/s$. The maximum value of the μ upper bound is 1.124 at $123.363\,rad/s$. Thus, the parametric robustness margin is : $\frac{1}{\max_\omega \bar{\mu}(\omega)} = 0.89\,(\pm 89\%)$. The

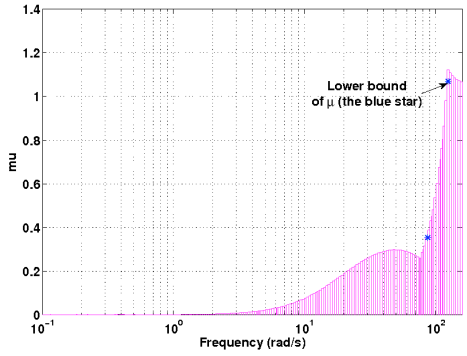

Fig. 9. μ response associated with the force feedback yoke for $J_y = 0.03 kg.m^2$ and $J_{a_0} = 1 kg.m^2$ nominal values.

blue star on the Fig. 9 represents the μ lower bound : $\max_\omega \underline{\mu}(\omega) = 1.07$ at $\omega = 124.354 rad/s$. The worst-case parametric configuration provided by μ-lower bound is :

$$\delta_{J_p}^{worst}(\omega) = 0.93,\ \delta_{J_a}^{worst}(\omega) = -0.93\,.$$

According to (3) : $J_a = 0.07\,kg.m^2$ and $J_p = 0.028\,kg.m^2$. This analysis confirms experiments : when the performance is high ($J_a = 0.07\,kg.m^2$ is lower than the main objective: $.1\,kg.m^2$), the robustness of pilot inertia is poor and justify unstablity encoutered during experiments with a pilot [10].

4. ROBUST STRUCTURED CONTROL H_∞

The main challenge **(objective #2)** of this robust controller is to provide robustness with respect to uncertainties of the pilot arm inertia J_p for a given performance J_a. This issue of coupling dynamics between pilot and an haptic interface had been intensely investigated [16]. In this paper, a simple H_∞ mixed sensitivity synthesis approach to design the position inner loop controller is considered. The H_∞ standard problem is depicted in Fig. 10. Such a design was considered by taking into account the previous results:

- robust stability problem appears around $120\,rd/s$, so a roll-off filter is required to attenuate the complementary sensitivity function and thus cut the high frequency of torque measurement;
- the position servo-loop bandwidth can be taken into account through a weight of the sensitivity function;
- transmission delays are quite determinant and must be taken into account in the design model;
- finally, the 3 measurements θ_y, θ_m and C_{mes} are considered as inputs of the new H_∞ controller.

Considering the nominal modal $G(s)$, delays and weighting functions, the order of the standard problem is order 11. In general, such an approach generates high order controller $K(s)$. Nonsmooth optimisation of structured H_∞ controller [20][21] available now in MATLAB toolbox is used to design a low 2^{nd} order controller. The weight on the sensitivity function "S" is defined by:

$$\mathcal{W}_1^{-1} = 1 - \frac{\omega_n^2}{s^2 + 2\zeta\omega_n s + \omega_n^2} = \frac{s^2 + 2\zeta\omega_n s}{s^2 + 2\zeta\omega_n s + \omega_n^2} \qquad (4)$$

The parameter ω_n determines the minimum bandwidth, while the damping coefficient ζ specifies the acceptable height of the peak of the sensitivity function. For an efficient important "Roll-off" attenuation, a second order filter $\mathcal{W}_2$ is specified ($i = 2$). Thus, specifications set out above are taken into account by the synthetic scheme shown in Fig. 10 (with ω_n=35 rad/s and $\omega = 900 rad/s$). First order PADE approximations are used to model the various delays.

In Fig 11, the obtained sensitivity function (S) and complementary function (KS), the weighting filters $\mathcal{W}_1^{-1}$ and $\mathcal{W}_2^{-1}$ are depicted. Note that, the templates are well respected since $\gamma = 1.09$. Thus, Fig 12 reveals that the reference admittance model is met in the frequency band $0-35 rad/s$ when the outer loop is closed. The corresponding second oreder controller $\mathcal{K}(s)$ is defined by:

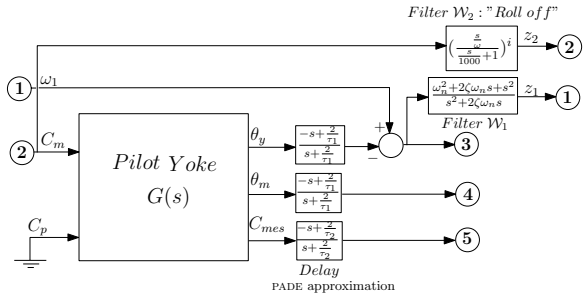

Fig. 10. Synthesis scheme H_∞.

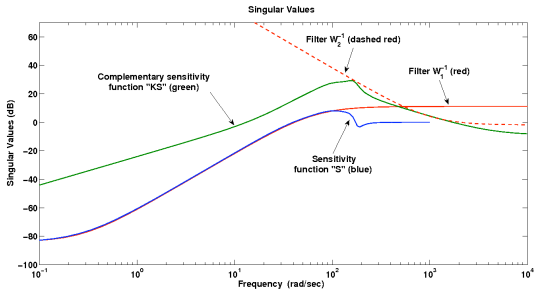

Fig. 11. Frequential response in performance ($\mathcal{W}_1^{-1}$) and robustness ($\mathcal{W}_2^{-1}$)

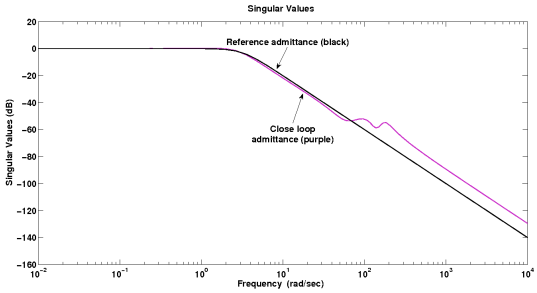

Fig. 12. Yoke admittance frequency-domain responses $\frac{\theta_y}{C_p}(s)$ for H_∞ control : admittance reference model $Y_{ref}(s) = 1/(0.1s^2 + 0.44s + 1)$ (black), closed loop with admittance reference model (purple).

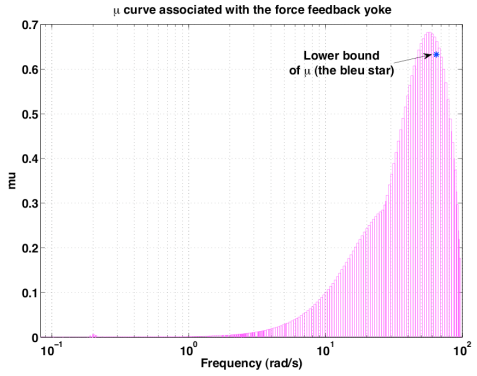

Fig. 13. μ curve associated with the force feedback yoke for $J_y = 0.03kg.m^2$ and $J_{a_0} = 1kg.m^2$ nominal values.

$$\mathcal{K} : \begin{cases} A = \begin{bmatrix} -14.85 & 388.1 \\ -1.099 & -120.8 \end{bmatrix} B = \begin{bmatrix} -1854 & -29.4 & 20.79 \\ 471 & 12.31 & 2.032 \end{bmatrix} \\ C = \begin{bmatrix} -0.03916 & 3.374 \end{bmatrix} D = \begin{bmatrix} 0.3516 & -0.3053 & -0.02547 \end{bmatrix} \end{cases} \quad (5)$$

4.1 Robustness analysis for nominal values

For $J_y = 0.03\,kg.m^2$ and $J_{a_0} = 1\,kg.m^2$ (nominal values), Fig. 13 plots μ upper and lowed bound responses on a mesh of 1000 points distributed between 0.1 and $200rad/s$. The maximum value of the μ upper bound is 0.682 in $58.13rad/s$. Thus, the parametric robustness margin is $\frac{1}{\max_\omega \bar{\mu}(\omega)} = 1.47\,(\pm 147\%)$. The blue star on the Fig. 13 represents the μ lower bound $\max_\omega \underline{\mu}(\omega) = 0.633$ at $\omega = 64.6rad/s$. The worst-case parametric configuration provided by μ-lower bound is :

$$\delta_{J_p}^{worst}(\omega) = 1.58,\ \delta_{J_a}^{worst}(\omega) = -1.58\ .$$

According to (3) $J_a = -0.58\,kg.m^2$ and $J_p = 0.0474\,kg.m^2$. Of course, J_a can not be negative. This result highlights that this design can support very low values for the apparent inertia J_a (till 0) with a quite good robustness against pilot inertia by comparison with the classical P.D. design.

4.2 Robustness analysis for performance objective

Fig. 14 shows the result of μ-analysis for $J_{a_0} = 0.1\,kg.m^2$ (performance objective) and $J_y = 0.03 + 58\% = 0.52\,kg.m^2$. Indeed, J_y is shifted to normalize $\delta_{J_p}^{worst}$ to 100% in the previous analysis . Fig. 14 plots μ upper and lower bound responses on a mesh of 1000 points distributed between 0.1 and $200rad/s$. The maximum value of the μ upper bound is 1.42 at $75.957rad/s$. Thus, the parametric robustness margin is $\frac{1}{\max_\omega \bar{\mu}(\omega)} = 0.7\,(\pm 70\%)$. The blue star on the Fig. 14 represents the μ lower bound : $\max_\omega \underline{\mu}(\omega) = 1.367$ at $\omega = 75.396rad/s$. The worst-case parametric configuration provided by μ-lower bound is :

$$\delta_{J_p}^{worst} = 0.73,\ \delta_{J_a}^{worst}(\omega) = -0.73\ .$$

According to (3) $J_a = 0.028\,kg.m^2$ and $J_p = 0.052\,(1 + 0.73) - 0.03 = 0.06\,kg.m^2$. The objective is achieved : when the performance is high ($J_a = 0.028\,kg.m^2$ is low w.r.t. the main objective: $0.1\,kg.m^2$) the robustness of pilot inertia is strong.

5. DYNAMIC COUPLING WITH CONTROL H_∞

The control structure proposed in section IV allows to achieve the objective (i.e. $J_a = 0.1kg.m^2$) and to have an yoke admittance very close to the reference model.

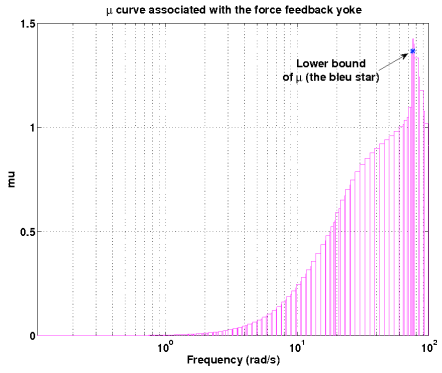

Fig. 14. μ curve associated with the force feedback yoke, $J_a = 0.1kg.m^2$ and $J_y = 0.03 + 58\%kg.m^2$.

The Fig. 15 shows the angular reference position of yoke (dashed blue line) when the pilot makes a solicitation (black line). The system is stable when the pilot clenches the yoke at $time = 5sec$ and when the pilot applies an periodic excitation (between 8 and $12sec$). The delay is now negligible ($0.05sec$) between $\theta_{ref}(t)$ and $\theta_y(t)$.

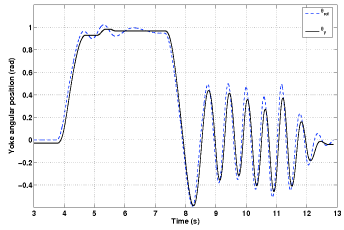

Fig. 15. Angular reference position of yoke (dashed blue) and angular position of yoke (black line) when the pilot makes a sollicitation : $Y_{ref}(s) = 1/(0.1s^2 + 0.44s + 1)$. The pilot applies a periodic excitation between 8 and 12 seconds.

6. CONCLUSION

In this article two different approaches had been presented to control the mechanical impedance of an aircraft yoke. Firstly, a classical PD approach has been implemented and revealed a low robustness to the pilot inertia. The performance (δ_{J_a}) and the robustness (δ_{J_p}) was evaluated using μ-analysis. This analysis confirms experiments : when the performance is high (that is when the prescribed apparent inertia is low), the robustness to pilot inertia J_p is poor. Secondly, a structured H_∞ controller has been developed. This approach allows a low order, easily implementable controller to be designed with a good performance/robustness trade-off. Both controllers were implemented on an experimental test-bed and the μ-analysis results were exprimentally validated with a pilot in the loop. Future works on this project will concern the use of robust control to generalize the control design to multi-degree of freedom control devices (side-stick).

REFERENCES

[1] K. Kong, H. Moon, B. Hwang, D. Jeon and M. Tomizuka, *"Impedance Compensation of SUBAR for Back-Drivable Force-Mode Actuation"*, IEEE Transactions on Robotics, vol.25, pp. 515-521, June 2009.

[2] Hogan and Neville, *"Impedance Control: An Approach to Manipulation"*, American Control Conference, pp. 304-313, June 1984.

[3] L. Barbe, B. Bayle, E. Laroche and M. de Mathelin, *"User adapted control of force feedback teleoperators: Evaluation and robustness analysis"*, IEEE/RSJ International Conference on Intelligent Robots and Systems, IROS 2008.

[4] A. Haddadi and Ke Hashtrudi-Zaad, *"Bounded-Impedance Absolute Stability of Bilateral Teleoperation Control Systems"*, IEEE Transactions on Haptics, vol. 3, pp. 15-27, March 2010.

[5] Laroche, E. and Barbe and, L. and Bayle, B. and de Mathelin, M., *"A methodology for identification of uncertain LFR model of the human operator for telemanipulation with force-feedback"*, Decision and Control (CDC), 2010 49th IEEE Conference on, 2010.

[6] X. Lamy, F. Colledani, F. Geffard, Y. Measson and G. Morel, *"Achieving efficient and stable comanipulation through adaptation to changes in human arm impedance"*, IEEE International Conference on Robotics and Automation, pp. 265-271, ICRA 2009.

[7] G.D. Glosser and W.S. Newman, *"The implementation of a natural admittance controller on an industrial manipulator"*, IEEE International Conference on Robotics and Automation, 1994.

[8] S.H. Kang, J. Maolin and P.H. Chang, *"A Solution to the Accuracy/Robustness Dilemma in Impedance Control"*, IEEE/ASME Transactions on Mechatronics , vol. 14, pp. 282-294, June 2009.

[9] F. Defay, D. Alazard and C. Antraygue, "Impedance Active Control of Flight Control Devices", *IEEE/ASME International Conference on Intelligent Robots and Systems*, AIM 2010.

[10] P. Latorre-Costa, F. Defay and D.Saussie, *"Preliminary Study of an Active Feedback System for Aircraft Guidance"*, *AIAA Guidance Navigation and Control Conferences*, Minneapolis (MN), 13-16 August, 2012.

[11] J.J Gil, A. Rubio and J.Savall "Decreasing the Apparent Inertia of an Impedance Haptic Device by Using Force Feedforward *IEEE Transactions on Control Systems Technology*, vol. 17, pp. 833-838, July 2009.

[12] E.C.Fritz, A.V Goran and R.Q van der linde, " Haptic Gripper with Adjustable Inherent Passive Properties", *In Proc. of EuroHaptics*, Munich Germany, June 5-7, 2004.

[13] CR.Carignan, KR.Cleary "Closed-loop force control for haptic simulation of virtual environment", Haptics-e, Vol 1,No. 2, Citeseer, 2000.

[14] M.Ueberle, M.Buss " Control of kinesthetic haptic interface", *In Proc. IEEE/RSJ International Conference on Robotics and Automation*, 2004.

[15] R.Koeppe, " Robot Compliant Motion based on Human Skill", *PhD thesis, Swiss Federal Institute of Technology*,2001.

[16] N. Bajinca, R. Cortes, M. Hauschild, "Robust Control for Steer-by-Wire Vehicles.", *Autonomous Robots 19, 193-214* 2005.

[17] N. Hogan, " Controlling impedance at the man/machine interface.", *Proceedings of the IEEE conference on Robotics and Automation*,1989.

[18] G. Ferreres "A practical approch to robustness analysis with aeronautical application", *Kluwer Academics/Plenum Press*, 1999.

[19] JM. Biannic, C. Doll, G. Ferreres, JF. Magni "Application et extensions de la μ-analyse", *Commandes robustes*, APII-JESA-35/2001, p. 9-32.

[20] P. Apkarian, V. Bompart, D. Noll, "Control Design in the Time and Frequency Domain using Nonsmooth Techniques.", *Systems and Control Letters- Elsevier*, 2008 .

[21] P. Apkarian, V. Bompart, D. Noll, "Time domain constrained H_∞ synthesis.", *International Journal of Control*, Volume 21, Issue 2, pp. 197-217, 25 January 2011.